Journal of Power Sources 190 (2009) 380–386

Contents lists available at ScienceDirect

Journal of Power Sources

journal homepage: www.elsevier.com/locate/jpowsour

A simple electric circuit model for proton exchange membrane fuel cells

Stavros Lazarou, Eleftheria Pyrgioti, Antonio T. Alexandridis*

Department of Electrical and Computer Engineering, University of Patras, Rion, 26500, Patras, Greece

ARTICLE INFO

Article history:
Received 14 May 2008
Received in revised form 4 December 2008
Accepted 18 January 2009
Available online 5 February 2009

Keywords:
Fuel cell
Distributed generation
PEM circuit model

ABSTRACT

A simple and novel dynamic circuit model for a proton exchange membrane (PEM) fuel cell suitable for the analysis and design of power systems is presented. The model takes into account phenomena like activation polarization, ohmic polarization, and mass transport effect present in a PEM fuel cell. The proposed circuit model includes three resistors to approach adequately these phenomena; however, since for the PEM dynamic performance connection or disconnection of an additional load is of crucial importance, the proposed model uses two saturable inductors accompanied by an ideal transformer to simulate the double layer charging effect during load step changes. To evaluate the effectiveness of the proposed model its dynamic performance under load step changes is simulated. Experimental results coming from a commercial PEM fuel cell module that uses hydrogen from a pressurized cylinder at the anode and atmospheric oxygen at the cathode, clearly verify the simulation results.

1. Introduction

Fuel cells are expected to play an important role in the power generation field by virtue of their inherently clean, efficient and reliable service. Their use is spreading widely and promising applications that include portable power, transportation, residential power and distributed power for utilities. Fuel cells are electrochemical devices that directly convert chemical energy in fuels into electrical energy. They promise power generation with high efficiency and low environmental impact with respect to most of the conventional power generators that use intermediate steps with heat production and conversion into mechanical work [1,2]. Therefore, the drawback of heat engines such as the thermodynamic limitation of the "Carnot" efficiency as well as the residues of combustion is avoided. On the other hand a main drawback of fuel cells that is hydrogen availability, it is currently solved by 'reforming' natural gas in hydrogen. However, for further deployment, fuel cells are required to become more competitive in terms of cost and hydrogen availability.

Among the various fuel cell types, the proton exchange membrane (PEM) fuel cell is drawing more attention due to its low operating temperature, ease of start-up and shut-down and compactness. Furthermore, the PEM fuel cell is being investigated as an alternate power generation system especially for distributed generation and transportation. The PEM fuel cell is providing reliable power at steady state; however, it is not able to respond promptly to a load step change. Since the fuel cell is an electrochemical energy conversion device that converts fuel into electricity, its dynamic behavior depends both on chemical and thermodynamic processes.

To obtain an efficient model for a PEM fuel cell for various applications is of paramount importance [3]. Various attempts have been made to model the proton exchange membrane fuel cell stack (PEMFCS) [4–8]. Many of the models proposed consist of mathematical equations which however are not adequately practical in power converter/system simulations. Although some of them are very accurate they are based on sophisticated geometries [9–13] that need millions of computational cells and tremendous CPU time for numerical simulations. Such large scale simulations could be conducted using only the parallel computing techniques and are far from the aim of the dynamic analysis needed for power systems applications. Circuit models are also used to represent the abstract dynamic behavior of a PEM fuel cell. The existing models however, among others need a parallel capacitor with extremely large values of about 3 F [14–16]. This may also lead to simulation failures depending on the dynamic situation; for example the time delay during the connection of an additional load is usually less than that during the disconnection. Recently, some other empirical models have been proposed [17,18]. Particularly in [17] a control-oriented model is presented that also needs a specific simulator software. In [18] a dynamic experimental model is developed by splitting the behavior into a nonlinear static and a linear dynamic subsystem, a so-called Uryson-Model.

In the current study, the merits of the most appropriate electric circuit models for power system analysis are considered. A novel and simple electric circuit model is proposed; the model includes simple electrical components that can be easily implemented in a circuit form. To simulate the proposed model, the Alternative Tran-

* Corresponding author. Tel.: +30 2610996893.
E-mail address: a.t.alexandridis@ece.upatras.gr (A.T. Alexandridis).

0378-7753/$ – see front matter © 2009 Elsevier B.V. All rights reserved.
doi:10.1016/j.jpowsour.2009.01.065

Nomenclature

act	activation
a, b	constant terms in Tafel equation ($V K^{-1}$)
E	reversible potential of each cell (V)
E_0	reference potential (V)
E_0°	standard reference potential (V)
F	Faraday's constant
H_2	hydrogen
H_2O	water
I, i	current (A)
I_{limit}	limitation current (A)
k_{RI}	empirical constant in calculating R_{ohmic} (ΩA^{-1})
k_{RT}	empirical constant in calculating R_{ohmic} (ΩK^{-1})
n	ideal transformer ratio ($n = 1$)
n_0	temperature invariant part of V_{act} (V)
ohm	ohmic
O_2	oxygen
p_i	partial pressure of species (Pa)
R	gas constant
R_i	resistance of type I (Ω)
T	temperature (K)
V	terminal voltage (V)
V_i	voltage drop of type (V)
z	number of electrons participating
*	effective value

sients Program–Electromagnetic Transients Program (ATP–EMTP) is used. It is implemented by lumped elements: one dc source and three resistors are needed to simulate the steady state behavior while one ideal transformer, two ideal diodes, and two nonlinear inductors is series with small resistors are used instead of large capacitors to simulate in detail the dynamic behavior. In order to accurately adjust the nonlinear characteristic of the inductors appeared in the proposed model, experimental data have been used.

Thus, the dynamic performance of a fuel cell is effectively approached through a simple circuit model although this performance is caused by a process of electrochemical and thermodynamic nature. Furthermore, the use of the two nonlinear inductors in the proposed model, overcomes the main problem of the existing circuit based model approaches, i.e. the different dynamic behavior of the fuel cell between a connection and a disconnection of a load. The main contribution of our work is that the proposed model can be used as an accurate, effective and easily applied tool in any circuit based analysis and design. Therefore the scientific and industrial benefits such as reduced CPU effort and direct implementation in any electric circuit simulation program become evident.

The paper is organized as follows. In Sections 2 and 3, all the steady state and dynamic characteristics of a fuel cell that we take into consideration in our model development, are analyzed. The development of the proposed model is presented in Section 4 while in Section 5, it is evaluated through simulation and experimental results. Both the worst dynamic conditions of a power load connection and disconnection are addressed. Finally, some conclusions are given in Section 6.

2. Steady state characteristics of a PEM fuel cell

The PEM fuel cell is very simple and uses a polymer (membrane) as the solid electrolyte and a platinum catalyst. The hydrogen from a pressurized cylinder enters the anode of the fuel cell and the atmospheric oxygen enters the cathode (Fig. 1). Protons and electrons

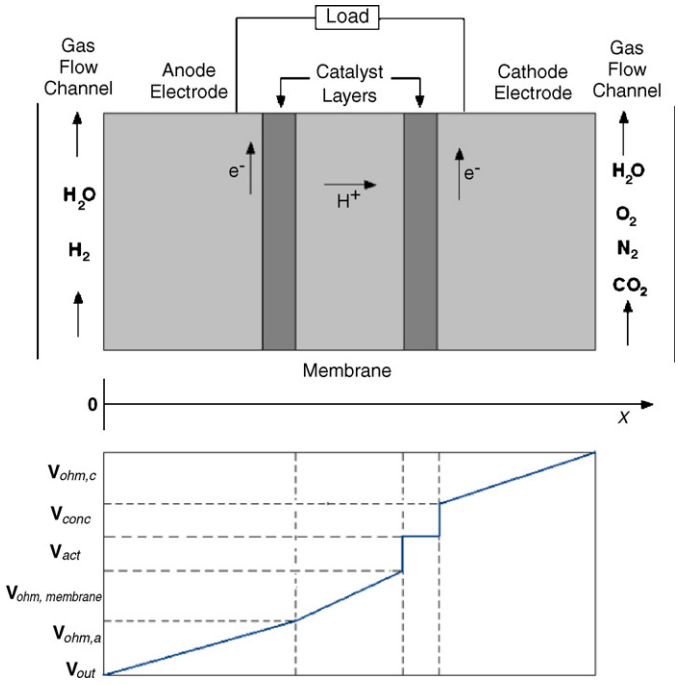

Fig. 1. Schematic diagram of a PEM fuel cell and voltage drops across it (redrawn from [13]).

are separated from hydrogen on the anode side. In a basic PEM cell, the protons are transported to the cathode side through the polymer and the electrons are conducted through the load outside the electrode [5]. A fuel cell stack is composed of several fuel cells connected in series separated by bipolar plates [4] and provides fairly large power at higher voltage and current levels.

Proton exchange membrane fuel cells combine hydrogen and oxygen over a platinum catalyst to produce electrochemical energy with water as the end-product. The steady state of an individual cell voltage is determined by the maximum cell voltage (or EMF) and the various voltage drops (losses) [19]. The ideal EMF is the maximum voltage that each cell in the stack can produce at a given temperature and a defined partial pressure of reactants and products. The losses, which are also called polarization, originate primarily from three sources: (a) activation polarization, (b) ohmic polarization, and (c) concentration (mass transport) polarization. Each of these is associated with a voltage drop and is dominant in a particular region of current density (low, medium, or high). Fig. 2 illustrates

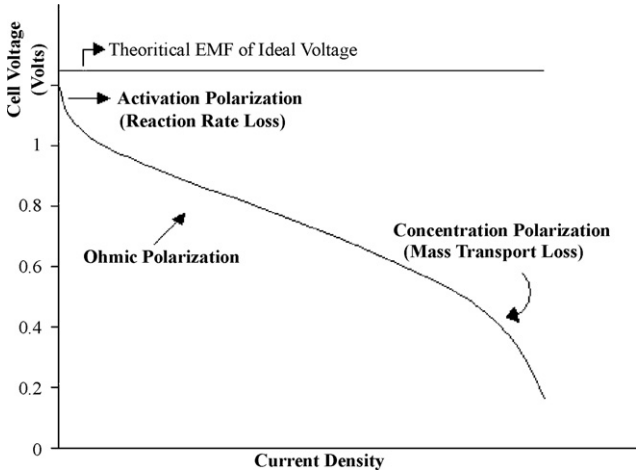

Fig. 2. V–I characteristic of a single PEM fuel cell (redrawn from [8]).

the different regions and the corresponding polarization effects of a typical single cell operating at room temperature and typical air pressure [19].

2.1. Electrochemical reaction and maximum fuel cell output voltage (EMF)

The electrochemical reaction in a PEM fuel cell can be simply written as

$$H_2 + \tfrac{1}{2}O_2 = H_2O_{(l)} \quad (1)$$

The fuel is humidified H_2 and the oxidant is humidified air. It is assumed that the effective anode water vapor pressure is 50% of the saturated vapor pressure while the effective cathode water pressure is 100%.

The thermodynamic potential of the reaction (1) is defined by the Nernst equation [20,21]:

$$E = E^\circ - \frac{RT}{nF}\ln[p^*_{H_2}\sqrt{(p^*_{O_2})}] \quad (2)$$

where E° represents a reference potential at unit activity, and the partial pressure terms correspond to oxygen and hydrogen concentrations. The standard state defines a standard state reference potential $E_0{}^\circ$ (equal to 1.229 V at 298.15 K and 1 atm), and E° will vary from the standard state reference in accordance with temperature [21]

$$E^\circ = E_0^\circ + (T - T_0)\left(\frac{\Delta S^\circ}{nF}\right) \quad (3)$$

where T_0 is the standard state temperature (298.15 K). The entropy change of a given reaction is approximately constant (the variation in specific heat with the expected changes in temperature is minimal) and can be set to the standard state value. Thus the reference potential varies directly with temperature [21] via the form

$$E^\circ = \beta_1 + \beta_2 T \quad \text{where} \quad (4)$$

$$\beta_1 = 1.229\,\text{V} - \frac{298.15\Delta S_0^\circ}{nF} \quad (5)$$

$$\beta_2 = \frac{\Delta S_0^\circ}{nF} \quad (6)$$

Using literature values for the standard-state entropy change, the value of β_2 in this equation can be calculated to be $-0.85\times10^{-3}\,\text{V K}^{-1}$ [21]. Eq. (2) can now be written as

$$E = 1.229 - 0.85\times10^{-3}(T - 298.15) - \frac{RT}{nF}\ln[p^*_{H_2}\sqrt{(p^*_{O_2})}] \quad (7)$$

Further expansion of this equation yields

$$E = 1.229 - 0.85\times10^{-3}(T - 298.15) - 4.3085\times10^{-3}T[\ln(p^*_{H_2}) + \tfrac{1}{2}\ln(p^*_{O_2})] \quad (8)$$

This voltage corresponds to one cell.

2.2. Polarization of a PEM fuel cell (activation-ohmic-concentration losses)

2.2.1. Activation polarization drop

The activation polarization loss (dominant at low current density) is present when the rate of the electrochemical reaction at the electrode surface is controlled by sluggish electrode kinetics [19]. Activation losses increase as the current increases. The activation losses can be obtained by Tafel equation.

$$V_{act} = \frac{RT}{azF}\ln\left(\frac{i}{i_0}\right) = T[a + b\ln(I)] \quad (9)$$

On the other hand, an empirical equation for V_{act} is given in [9], where a constant (n_0) is added to (9) as follows:

$$V_{act} = n_0 + (T - 298)a + Tb\ln(I) = V_{act1} + V_{act2} \quad (10)$$

where $V_{act1} = n_0 + (T - 298)a$ is the voltage drop affected only by the fuel cell internal temperature, while $V_{act2} = Tb\ln(I)$ is both current and temperature dependent.

The equivalent resistance of activation corresponding to V_{act2} is defined as:

$$R_{act} = \frac{V_{act2}}{I} = \frac{Tb\ln(I)}{I} \quad (11)$$

2.2.2. Ohmic polarization (loss)

The ohmic loss is associated with the resistance of the polymer electrolyte membrane to the ions and the resistance of imperfect electrodes. The loss (voltage drop) in the fuel cell is approximately linear in this region and can be expressed as:

$$V_{ohm} = V_{ohm,a} + V_{ohm,membrane} + V_{ohm,c} = IR_{ohm} \quad (12)$$

where R_{ohm} is also a function of current and temperature [9]

$$R_{ohm} = R_{ohm0} + k_{RI}I + k_{RT}T \quad (13)$$

where R_{ohm0} is the constant part of the R_{ohm}.

2.2.3. Concentration polarization (mass transportation losses)

The concentration polarization is related to the change in concentration of the reactants at the surface of the electrodes as the fuel (hydrogen) is depleted. The fuel and oxidant concentrations are less at the areas of the fuel gas channels compared to the inlet portion of the stack. This loss becomes significant at higher currents when the fuel and oxidant are depleted at higher rates and the concentration in the gas channel is at a minimum.

In general, the mass transportation (transfer) losses are given by [1,22]:

$$V_{conc} = -\frac{RT}{zF}\ln\left(1 - \frac{I}{I_{limit}}\right) \quad (14)$$

The equivalent resistance for the concentration loss is:

$$R_{conc} = \frac{V_{conc}}{I} = -\frac{RT}{zFI}\ln\left(1 - \frac{I}{I_{limit}}\right) \quad (15)$$

For the PEMFC that operates on pure hydrogen and atmospheric air the ideal voltage can be calculated based on Gibbs free energy and is equal to 1.2 V at 25 °C and atmospheric pressure for a single fuel cell [19]. A higher output voltage is obtained by connecting several cells in series. The area of the cell determines the output current.

3. Dynamic response of a PEM fuel cell

The dynamic response of fuel cells to load change is important for cell start-up and automotive applications. Three major transient processes are responsible for the dynamic characteristic of a PEM fuel cell, namely, (i) reactant gas transport in the channel and porous media, (ii) membrane hydration and dehydration, and (iii) formation and discharging of the charge double layer [23]. The time constant for a reactant gas to transport through gas diffusion layer (GDL) can be estimated simply by its diffusion time, i.e. δ^2_{GDL}/D_g. This gives a time constant between 0.1 and 1 s. The slowest process, however, is membrane hydration, the time constant of which can be estimated by [23]

$$\frac{(\rho\delta_m\Delta\lambda)/(EW)}{I/(2F)} \quad (16)$$

λ is the membrane hydration, ρ the density, D_g the diffusion coefficient, δ_m the membrane thickness, δ_{GDL} the GDL thickness, EW the

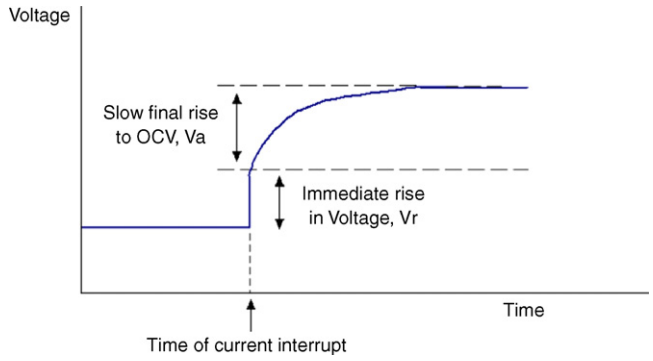

Fig. 3. Sketch graph of voltage against time for a fuel cell after a current interrupt.

equivalent weight, and F is the Faraday's constant. This is to assume that a dry membrane is hydrated by production water generated at the current density, I. For Nafion 112 and a reference current density of 1 A cm^{-2}, this is about 25 s! Therefore, for low humidity cells where the membrane undergoes water content changes, the water accumulation term is essential for transient analyses [23,24]. Detailed transient models are also developed to study the response of a single cell to dynamic load change. Um et al. [9] were one of the first to study this response of a PEFC to a voltage step change. Due to the fully humidified gas feed on the anode and cathode, the membrane hydration process no longer contributed to the cell transients; as such, it was sufficient to include gas-transport transients under these fully humidified conditions.

The formation and discharging of the charge double layer according to [14] is a complex and interesting electrode phenomenon, and whole books have been written on the topic [25].

3.1. The double layer charging effect

In this paper the novel proposed electric model is based at the 'charge double layer' phenomenon, which is important in understanding the dynamic electrical behavior of fuel cells. In a PEM fuel cell, the two electrodes are separated by a solid membrane (Fig. 2) which only allows the H^+ ions to pass, but blocks the electron flow [1,14]. The electrons will flow from the anode through the external load and gather at the surface of the cathode, to which the protons of hydrogen will be attracted at the same time. Thus, two charged layers of opposite polarity are formed across the boundary between the porous cathode and the membrane [14,26]. The layers, known as electrochemical double layer, can store electrical energy and behave like a super capacitor. Generally speaking, the effect of this capacitance, resulting from the charge double layer, gives the fuel cell a smooth dynamic response in the sense that the voltage reaches the new value in response to a change in current demand.

The current interrupt technique [14] can be used to give accurate quantitative results. It can be performed using standard low-cost electronic equipment. Suppose a cell is providing a current at which the concentration (or mass transport) overvoltage is negligible. The ohmic losses and the activation overvoltage will in this case cause the voltage drop. Suppose now that the current is suddenly cut off. The charge double layer will take some time to disperse (The time constant of double layer discharging is between micro- and milliseconds.), and so will the associated overvoltage. However, the ohmic losses will immediately reduce to zero. We would therefore expect the voltage to change as in Fig. 3 [14] if the load was suddenly disconnected from the cell. Fuel cell's performance during the connection of a load is almost the same. Fuel cell produces additional delays which are available during the field measurements.

3.2. In the field measurements

Experimental data were obtained from a Nexa® power module 1.2 kW [27], manufactured by Ballard Power. The test set-up included the fuel cell, a compressed pure hydrogen tank, a Tektronix DPO4104 oscilloscope and a load resistant rated from 0 to 100 Ω. The test arrangement is fully controlled by personal computer and connected to the Internet for distant handling.

The module is a fully integrated system that produces unregulated dc power from a supply of hydrogen (fixed pressure of 72 psi) and air. It has a rated power of 1200 W. The output voltage varies from 43 V dc at open circuit to about 26 V dc at rated current (46 A). The load current was varied from a small value to a maximum of 70 A. To validate the proposed model, several experiments were conducted on the commercial fuel cell module.

The experiments contain the current interrupt technique and the connection of a load. The measured time is the average essential time for the fuel cell, to stabilize its output voltage, after the change of the load. Aim of the experiments is to estimate the transient behavior of the fuel cell module after the change of its load. The experimental results are shown in Fig. 4. In order to be understandable the time delay τ is fitted to typical curves with respect to

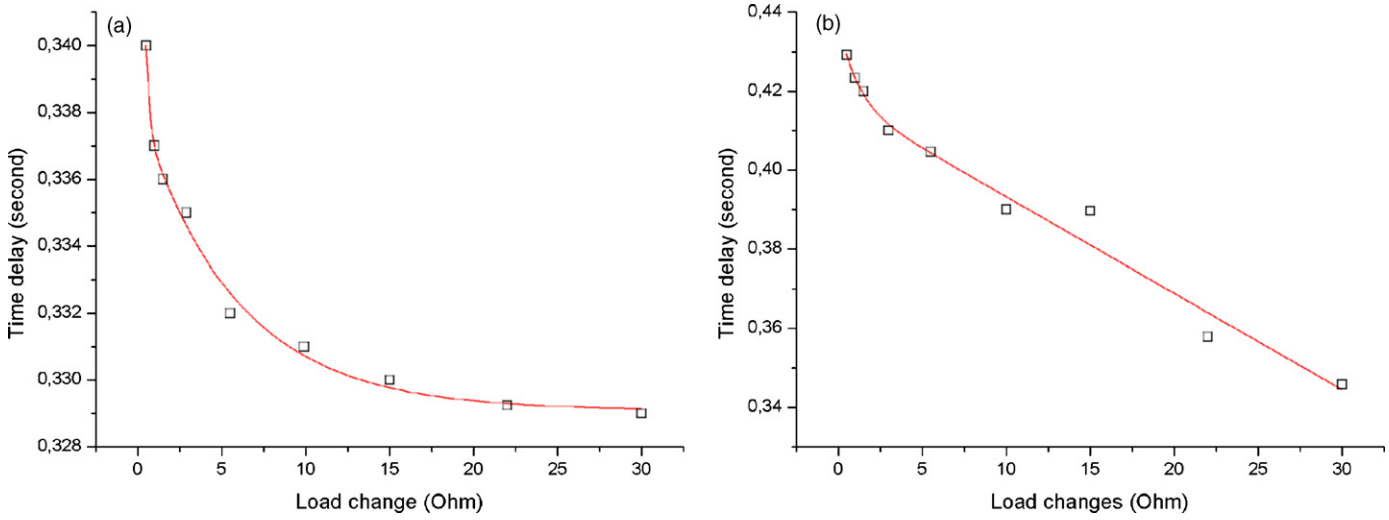

Fig. 4. Experimental results. (a) Average time needed for the fuel cell to stabilize its output voltage during the connection of a load [17]. (b) Average time needed for the fuel cell to stabilize its output voltage during the disconnection of a load [18] (current interrupt technique).

Table 1
Constant and variable parameters' ranges.

E_0°	1.229 V at 298.15 K and 1 atm or
T	298.15–368.15 K
T_0	298.15 K
F	96487 C mol^{-1}
R	8.3143 J (mol K)$^{-1}$
$p^*_{O_2}$	2.2 psig for air oxidant
$p^*_{H_2}$	5.0 psig
β_1	1.482 V
β_2	-0.85×10^{-3} V K^{-1}
V_{act1}	$1.2581I - 1.6777 \times 10^{-6}I^6 + 1.2232 \times 10^{-4}I^5 - 3.4 \times 10^{-3}I^4 + 0.04545I^3 - 0.3116I^2$
V_{act2}	$0.00112 \times (T - 298)I$
R_{ohm0}	0.2793 Ω
k_{RI}	0.001872
k_{RT}	$-0.0023712 + 0.7066/T$
R_{conc}	$0.080312 + 5.2211 \times 10^{-8}I^6 - 3.4578 \times 10^{-6}I^5 + 8.6437 \times 10^{-5}I^4 - 0.010089I^3 + 0.005554I^2 - 0.010542I$

the load changes r, as follows

$$\tau(t) = 0.00909e^{-(r/5.77048)} + 0.02763e^{-(r/0.21061)} + 0.3291 \quad (17)$$

$$\tau(t) = 0.0208e^{-(r/1.06614)} + 3331.3088e^{-(r/1.3661\times10^6)} - 3330.89077 \quad (18)$$

According to Fig. 4 and Eqs. (17) and (18) the time delay is clearly different during the connection or disconnection of an additional load.

Table 1 presents the constants and parameters introduced in Sections 2 and 3.

4. Model development

In this section, the proposed circuit based model is developed. To this end, all the steady state and dynamic assumptions presented in the previous two sections are taken into account.

Particularly, for the steady state performance, activation loss, ohmic resistance voltage drop, and concentration overpotential are voltage drops across the fuel cell (see Fig. 2 and Ref. [1]). Therefore:

$$V_{cell} = E_{cell} - V_{act,cell} - V_{ohm,cell} - V_{conc,cell} \quad (19)$$

Because parameters for individual cells can be lumped together to represent a fuel-cell stack, the output voltage of the fuel cell stack can be obtained as:

$$V_{out} = N_{cell}V_{cell} = E - V_{act} - V_{ohm} - V_{conc} = E - (R_{act} + R_{ohm} + R_{conc})I \quad (20)$$

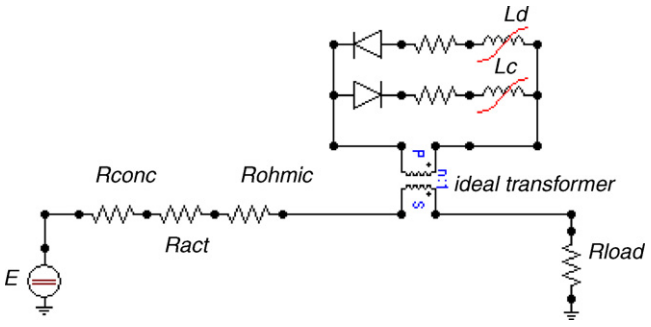

Fig. 5. The fuel cell equivalent circuit model proposed at this paper.

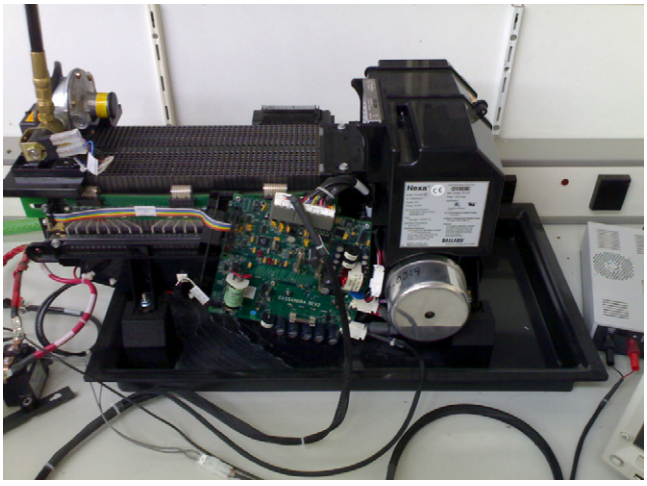

Fig. 6. 1.2 kW Nexa power module.

The E is calculated from Eq. (8). The R_{act} is calculated from Eq. (11) while the R_{ohmic} and the R_{conc} are calculated from the Eqs. (13) and (15), respectively.

In the case where the fuel cell operates at a definite operation point, one can obviously assume

$$R^* = R_{conc} + R_{act} + R_{ohmic} = ct \quad (21)$$

For the dynamic performance, it is well known that the existing circuit methods for the simulation of a fuel cell, use capacitors with extremely large values, about 3 F, connected in parallel to the model [15,16]. These models cannot simulate the time differences between the disconnection (current interrupt technique [14]) and the connection of a load. At this paper is presented an alternative technique that uses two saturable inductors to overcome this problem. The saturable inductors introduce the suitable delays appeared. The diodes drive the current to the inductor L_c or L_d properly during the connection or the disconnection of an additional load. Therefore, the differences appeared during connection and disconnection of a load can be accurately represented. The resistors beside the saturable inductor are very small and are used to further adjust the dynamic behavior of the model with that obtained experimentally.

For every operational point the two current/flux characteristic for the nonlinear inductors are derived from (17) and (18).

Fig. 5 shows the proposed circuit model of a commercial PEMFC module. For the simulation of the proposed model Alternative Transients Program – Electromagnetic Transients Program is used. The complete circuit is developed by modeling the different operating regions using elements from the ATP–EMTP simulation library.

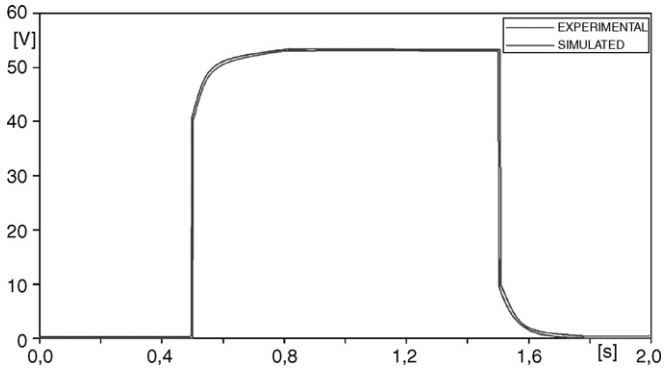

Fig. 7. Simulated and measured results compared for a certain operational point.

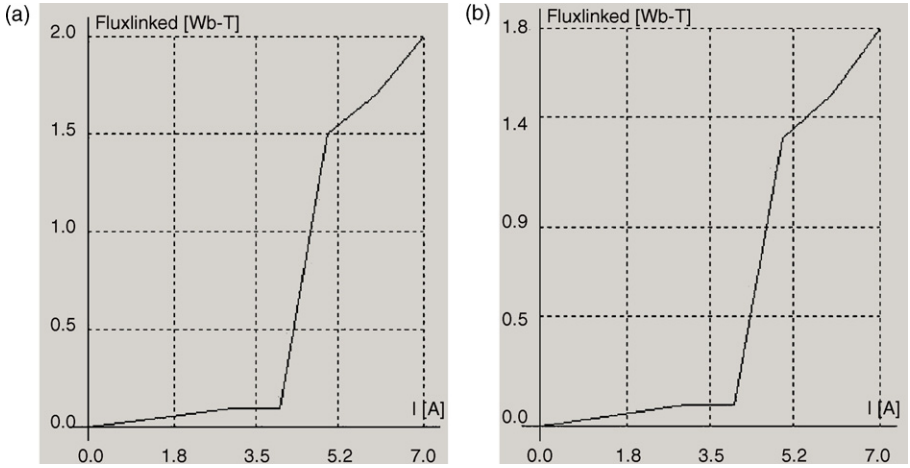

Fig. 8. Characteristics of the saturated inductors. (a) For the induction L_c operating during the connection of additional load. (b) For the induction L_d operating during the disconnection of additional load.

ATP–EMTP is a universal commercial program for digital simulation of transient phenomena of electromagnetic as well as electromechanical nature. With this digital program, complex networks and control systems of arbitrary structure can be simulated. ATP–EMTP has extensive modeling capabilities and additional important features besides the computation of transients. It has been continuously developed through international contributions over the past 20 years. ATP-Draw is the ATP–EMTP's graphic user interface. In this environment the proposed model was formulated by one dc type 11 source, five resistors, one ideal transformer, two ideal diodes, and two nonlinear type 93 inductors. The transformer's ratio was selected to be one ($n = 1$). As it is shown in Fig. 3 during connection or disconnection the nonlinear inductors should be initially approximately zero and progressively take their final values. The matching of the nonlinear characteristics of the inductors used is based on the experimental results. In this frame, the proposed model was created to be a part of an integrated platform deployed to optimize the installation of distributed generation at medium voltage networks [29,30].

5. Results and discussion

In order to validate the proposed model, simulated and experimental results are obtained and compared. To this end, Nexa® power module 1.2 kW, manufactured by Ballard Power is used as shown in Fig. 6.

The module is a fully integrated system that produces unregulated dc power from a supply of hydrogen (fixed pressure of 72 psi) and air. It has a rated power of 1200 W. The output voltage varies from 43 V dc at open circuit to about 26 V dc at rated current (46 A). The load current was varied from several amperes to a maximum of 70 A. The automated operation is maintained by an embedded controller board. Some tests were performed by electrically isolating the PEM stack from the controller board to obtain pure stack data. In according to the manufacture's procedure, after starting the fuel cell system if any of the start-up criteria is not met during the staring period, the system fails and stops. To make the fuel cell stack ready for the experiment in order to achieve pure results, power isolation is accomplished by connecting the controller board to an external power supply.

To validate the proposed model, several experiments were conducted on the commercial fuel cell module. The experiments contain the current interrupt technique and the connection of a load. The measured time is the average essential time for the fuel cell, to stabilize its output voltage, after the change of the load. Aim of the experiments is to estimate the transient behavior of the fuel cell module after the change of its load. Once the stack finished its operation, it was cooled down close to room temperature in about 20 min with no external load. This is an acceptable condition for the Nexa power module to be shut off. The supply pressures to the stack were 5.0 psig for hydrogen fuel and 2.2 psig for air oxidant. The fuel cell system was air cooled and had an attached humidity exchanger using exhaust water as a humidity resource [27,28].

In Fig. 7, one can see that at the time-instant $t = 0.5$ s a load $R_l = 20\ \Omega$ is connected. This caused a time delay is $t_d = 0.28$ s for the fuel cell. At the time-instant $t = 1.5$ s this load is disconnected. This caused a time delay is $t_d = 0.32$ s. For the selected inductors L_c, L_d characteristics, presented in Fig. 8, one can clearly observe that the simulated response is almost the same as the experimental one.

At this point we note that the proposed electric circuit model can effectively simulate any other type of fuel cell under appropriate adjustment of the values of its electric circuit components.

6. Conclusions

A novel circuit model for the PEM fuel cell stack is presented. The main contribution of this work is that the proposed model uses simple lumped electric circuit elements, i.e. resistors and saturable inductors. Especially, the two saturable nonlinear induction components, each used for the case of connection or the disconnection of an additional load, can guarantee the development of an accurate dynamic model that can be easily used in power system analysis and design. Although simple, the model can effectively represent the dynamic behavior of a PEM fuel cell that appears to have an initially rapid response following by a time delaying response. Experimental results obtained on a commercial fuel cell module verify the simulation results obtained by the proposed model.

Acknowledgments

The research for this study was financed by the European Union (75%) and the Greek Government (25%) [PENED 2003, code number 03ED158]. The authors are grateful to the reviewers for their valuable suggestions that made possible the improvement of the paper.

References

[1] DEO of Fossil Energy, National Energy Technology Lab., Fuel cell Handbook, seventh edition, EG&G Services, Parsons Inc., November 2004, Chapter 1 & 3.

[2] D.P. Wilkinson, N. St-Pierre, in: W. Vielstich, H. Gasteiger, A. Lamm (Eds.), Handbook of Fuel Cells—Fundamentals Technology and Applications, John Wiley and Sons, 2003.
[3] J. Stumper, C. Stone, J. Power Sources 176 (2008) 468–476.
[4] J.B. van der Merwe, C. Turpin, T. Meynard, B. Lafage, Proceedings of the IEEE Power Electronics Specialists Conference, 2002, pp. 333–338.
[5] S. Yerramalla, A. Davari, A. Feliachi, Proceedings of the IEEE Power Engineering Society Summer Meeting, vol. 1, 2002, pp. 82–86.
[6] K. Dannenberg, P. Ekdunge, G. Lindbergh, J. Appl. Electrochem. 30 (2000) 1377–1387.
[7] A. Kazim, H.T. Liu, P. Forges, J. Appl. Electrochem. 29 (1999) 1409–1416.
[8] G. Maggio, V. Recupero, L. Pino, J. Power Sources 101 (2001) 257–286.
[9] S. Um, C.Y. Wang, K.S. Chen, J. Electrochem. Soc. 147 (2000) 4485–4493.
[10] J.C. Amphlett, R.M. Baumert, R.F. Mann, B.A. Peppley, P.R. Roberge, J. Electrochem. Soc. 142 (I) (1995) 1–8.
[11] C. Martınez Baca, R. Travis, M. Bangb, J. Power Sources 178 (2008) 269–281.
[12] P.C. Sui, S. Kumarb, N. Djilali, J. Power Sources 180 (2008) 410–422.
[13] P.C. Sui, S. Kumarb, N. Djilali, J. Power Sources 180 (2008) 423–432.
[14] J. Larminie, A. Dicks, Fuel Cell Systems Explained, second edition, Wiley, UK, 2003.
[15] D. Yu, S. Yuvarajan, J. Power Sources 142 (2005) 238–242.
[16] S. Lazarou, K. Karavotas, E. Pyrgioti, A. Alexandridis, IASTED International Conference on Power and Energy Systems (EuroPES 2008), Corfu, Greece, June 2008.
[17] A.J. del Real, A. Arce, C. Bordons, J. Power Sources 173 (2007) 310–324.
[18] M. Meiler, O. Schmid, M. Schudy, E.P. Hofer, J. Power Sources 176 (2008) 523–528.
[19] National Energy Technology Laboratory, Fuel Cell Hand Book, sixth edition, 2002, pp. 2–9.
[20] M.W. Verbrugge, D.M. Bernardi, AIChE J. 37 (1991) 1151–1163.
[21] C. Berger, Handbook of Fuel Cell Technology, Prentice Hall, Englewood Cliffs, NJ, 1968.
[22] C. Wang, M.H. Nehrir, S.R. Shaw, IEEE Trans. Energy Convers. 20 (June (2)) (2005) 442–451.
[23] C.Y. Wang, Chem. Rev. 104 (2004) 4727–4766.
[24] N. Sammes (Ed.), Fuel Cell Technology—Reaching Towards Commercialization, Springer, USA, 2006.
[25] J.O'M. Bockris, B.E. Conway, E. Yeager (Eds.), Comprehensive Treatment of Electrochemistry, vol. 1, Plenum Press, New York, 1975.
[26] M.T. Iqbal, Renew. Energy 28 (April (4)) (2003) 511–522.
[27] Ballard Power System, Nexa Power Module Integration Guide, 2007.
[28] W. Zhu, R. Payne, D. Cahela, B. Tatarchuk, J. Power Sources 128 (2004) 231–238.
[29] S. Lazarou, E. Pyrgioti, Int. J. Electr. Comput. Eng. I (4) (2007) 468–478.
[30] S. Lazarou, G. Marmidis, E. Pyrgioti, 29th International Conference on Lightning Protection (ICLP 2008) Uppsala, Sweden, June 2008.